CFD ANALYSIS AND EXPERIMENTAL INVESTIGATION OF HEAT TRANSFER AND FLUID FLOW IN A PARABOLIC TROUGH SOLAR COLLECTORUSING TWISTED TAPE INSERTS AND HYBRID NANOFLUIDS

[1]R. Vasanthi, [2]G. Jaya Chandra Reddy

1. Research scholar, YSR Engineering college of Yogi vemana university, AP,
Email: vasanthi.vennapusa@gmail.com .
2. Professor, YSR Engineering college of Yogi vemana university, AP, Email: jcr.yvuce@gmail.com.

ABSTRACT

This study was aimed to examine the effect of hybrid nanofluid on the thermal performance of Parabolic Trough Solar Collector (PTSC) was investigated. The simulation process was performed using Computational Fluid Dynamic (CFD).Nano technology plays very important role in the heat transfer solar applications, when used as a working fluid in parabolic collector enhances its efficiency due to its improved thermo-physical properties like thermal conductivity, heat capacity, density and viscosity. In order to achieve better heat transfer rate this can be done by changing the nature and properties of working fluids by introducing flow inserts is a common passive technique for enhancing the thermal performance of parabolic trough solar collectors. Nano fluids are a suspension of nano particles in a base fluid like water, ethylene glycol. In this paper both experimental and computational fluid dynamics study has been presented. Hybrid nanofluid possess enhanced thermal conductivity and better heat transfer coefficient as compared to the base fluid. Hybrid Nano fluid used is 0.5% (30% GO +70%TiO_2) - H_2O (DI). System performance is conducted under mass flow rate of 0.05kg/s. In ANSYS FLUENT 14.5 based computational fluid dynamics tool, the absorber tube is modeled as metallic stainless steel tube with working fluid flowing in it. Hybrid nanofluid is simulated using one-phase modeling techniques, while solar load cell and solar ray tracing are used for modelling the solar fluxes. Solar load model has been used for modeling solar fluxes. S2S radiation model has been used for modeling heat transfer comprising of conduction, convection and radiation. It has been reported from both experimental and CFD analysis that system performance is enhanced by using hybrid nano fluid as working fluid as compared with conventional fluid likes water. Also both experimental and CFD simulated data gives good result agreement.

KEYWORDS: Computational fluid dynamics, efficiency, Nano fluid, parabolic solar collector.

I. INTRODUCTION

Heat transfer enhancement or intensification is the study of improved heat transfer performance. Recently adequate energy source and material costs have provided significant resources for the development of enhanced energy efficient heat exchangers. As aresult, considerable emphasis has been placed on the development of various augmented heat transfer surfaces and devices. Anenhanced surface is more efficient in transferring heat than what might be called as a standard surface. While considering the associated flow friction change is also to be taken into account. Analogies between momentum and heat transfer show that increasing the friction factor increases the heat transfer coefficient. The moody chart shows that in turbulent flow increasing the relative roughness of the surface increases the friction factor. This chart is based on the random sand grain type of source roughness. Surface roughness can be produced by the machining of the surface as well as casing, forming, and welding processes. Other types of surface have been produced, and their friction factors and heat transfer characteristics have been tested for possible use in heat transfer augmentation. The use of fins on the outer surface of tube enhance heat transfer is well known. Internally finned tubes have been used also to enhance heat transfer to fluids flowing inside tubes. Heat transfer and friction factor correlations have been presented for internally finned tubes under laminar and turbulent flow conditions. Enhancement devices such as twisted taps have been employed in the form of inserts into the tubes to promote increased heat transfer for the laminar and turbulent flow of viscous fluid. Coiled tubes can serve as a heat transfer enhancement device because the secondary flow produced by the curvature causes an increase in the heat transfer coefficient. In general, enhancing the heat transfer can be divided into two groups. Passive method, without stimulation by the external power such as a surface coating, rough surfaces, extended surfaces, swirl flow devices, the convoluted (twisted) tube, additives for liquid and gases. The other is the active method, which requires extra external power sources, for example, mechanical aids, surface-fluid vibration, injection and suction of the fluid, jet impingement, and use of electrostatic fields. Passive heat transfer enhancement techniques (for example, wall roughness, swirl flow inducement, and inserts) are preferred over active (for example, surface vibration, electro-static fields) ones to obtain more compact heat exchangers and to reduce energy costs. The increasing heat transfer with augmentation is accompanied by an increase in the friction factor. In some situations the heat transfer coefficients are increased at most about 4 times while the friction factors are increased as much as 50% or more. An increased friction factor implies an increased power for pumping the fluid. For a given enhancement technique, if the heat transfer and the friction factor data are available as a function of the Reynolds number, it may be possible to optimize the system to reduce the heat transfer surface, to obtain increased heat transfer capacity and to reduce the power required for pumping the fluid.

The great attempt on utilizing different methods is to increase the heat transfer rate through the compulsory forced convection. Meanwhile, it is found that this way can reduce the sizes of the heat exchanger device and save up the energy. Heat transfer enhancement is characterized by rigorous research activities both in academic and industrial levels. (Prasad and Shen, 1993proposed a new criterion for evaluating the effectiveness of a passive heat transfer enhancement device. (Prasad and Shen, 1994) studied the enhancement of heat transfer by using several coil-wire inserts based on exergy analysis. Twelve different coil-wire inserts were tested in turbulent flow regions. (Ravigururajan and Bergles, 1996) presented the general correlations for the friction factor and heat-transfer coefficient for the single-phase turbulent flow in internally augmented tubes. Different types of commercial ribbed tubes were tested under heating conditions. (Agrawaletal. 1998) experimentally studied the heat transfer enhancement by coiled wire inserts during the forced convection condensation of R-22 inside horizontal tubes. Three different wire diameters and three different coil pitches were used in full length of the test-condenser. (Kim et al. 2001 visualized the flow pattern, void fraction and slug rise velocity on the counter-current two-phase flow in a vertical round tube with coil-wire inserts. (Wang and Sund, 2002) studied the heat transfer enhancement technology in the heat exchanger. (Rahai and Wong, 2002) experimentally studied the turbulent jets from round tubes with coil inserts. Recently, (V. Ozceyhan, 2005) numerically studied the conjugate heat transfer and thermal stress in the tube with coil-wire inserted tube under uniform wall heat flux. A finite difference scheme was employed to solve the energy and governing flow equations. Compared to a smooth tube, internal spiral grooves impart swirl to the essentially axial flow in the vicinity of the tube wall as well as provide benefits of surface roughness (groove height is typically smaller than the laminar sub-layer thickness in a turbulent flow) (Webb et al. 2000). Probably (Choi, 1995) at the Argonne National Laboratory was the first to employ particles of nanometer dimension suspended in solution as nanofluid and showed considerable increase in the nanofluid thermal conductivity.

(Yun et al. 2007) also reported the same observations in their study of flow boiling heat transfer characteristics of nitrogen in coiled wire inserted tubes. The Experimental investigations of Hsieh and Liu report that Nusseltnumbers were between four and two times of the bare tube at low Re number value. The present study attempts to theoretically investigate the heat transfer characteristics and friction factor of hybrid nanofluid flowing through a horizontally circular tube with different inserts like a twisted stripwing inserts. Previous studies have not been addressed heat transfer in tubes with such twisted stripwing insertsthrough the range of turbulent flow regime. Initially the CFD experiment is carried out with DI water as the moving fluid through pipe section without any inserts. With Insert: Two geometries of inserts are considered for CFD analysis i.e. Plane twisted wing insert and Horizontal left right twisted wing insert.

2. COMPUTATIONAL FLUID DYNAMICS MODELING

CFD provides numerical approximation to the equations that govern fluid motion. Application of the CFD to analyze a fluid problem requires the following steps. First, the mathematical equations describing the fluid flow are written. These are usually a set of partial differential equations. These equations are then discretized to produce a numerical analogue of the equations. The domain is then divided into small grids or elements. Finally, the initial conditions and the boundary conditions of the specific problem are used to solve these equations. The solution method can be direct or iterative. In addition, certain control parameters are used to control the convergence, stability, and accuracy of the method. All CFD codes contain three main elements: (1) A pre-processor, which is used to input the problem geometry, generate the grid, and define the flow parameter and the boundary conditions to the code. (2) A flow solver, which is used to solve the governing equations of the flow subject to the conditions provided. (3) A postprocessor, which is used to massage the data and show the results in graphical and easy to read format.

The equations governing the fluid motion are the three fundamental principles of mass, momentum, and energy conservation.

Continuity Equation

$$\frac{\partial u}{\partial t} + div(\rho u) = 0 \qquad (1)$$

ρ-Density, u- velocity, t-time

Momentum Equation:

$$\frac{\partial}{\partial t}(\rho u_i) + div(\rho u_i u) = -\frac{\partial p}{\partial x_i} + div(\mu grad u_i) \qquad (2)$$

P-Pressure, μ- viscosity

Energy Equation:

$$\frac{\partial}{\partial t}(\rho u_i) + div(\rho u_i u) = -Pdivu + div(kgradT) + \emptyset + S_i \qquad (3)$$

k-Thermal conductivity, T –temperature, ϕ-dissipation term, S-Source.

where ρ is the fluid density, *U* is the fluid velocity vector, μ is the viscous stress tensor, *p* is pressure, F is the body forces, E is the internal energy, *Q* is the heat source term, *t* is time, $S_h$is the dissipation term, and .q is the heat loss by conduction.

2.1. COMPUTATIONAL FLUID DYNAMICS METHODOLOGY

2.1.1. Geometric Modeling: Firstly, the 3-D geometry of the collector element is created. The geometry consists of two concentric cylinders with two fluid regions for the working fluid (inner cylinder) and the outer region (annulus). In the present analysis, the geometry is considered to be oriented along the z-axis,

with positive Z denoting the south direction while the positive X denotes the east direction. Upper part is mainly incident by incoming solar radiation while lower part is incident by reflected and concentrated solar radiation with the help of mirror reflector.

Fig:1: Geometrical modelling of Absorber tube with inserted twisted tapes

2.1.2. Material Models: In ANSYS FLUENT 14.5, material model is applied. In material model, various thermo physical properties of the materials are specified. Material models are applied for carrying out CFD simulation of GO+TiO_2 – H_2O (DI) Nano fluid based collector. Table -1 shows the material used along with their thermo-physical properties.

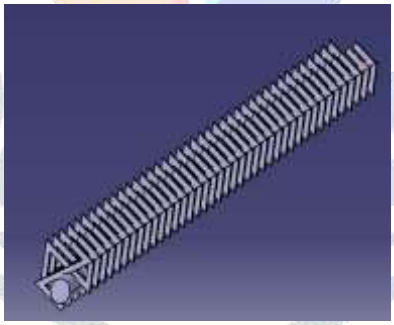

Table - 1. Thermo-physical properties

Thermo-physical properties	Water	GO-Water based Nano fluid (0.5% conc)	TiO_2-Water based Nano fluid (0.5% conc)	GO+TiO_2-Water based Nano fluid (0.5% conc)
Density(Kg/m^3)	1000	1054	1032	1086
Specific heat (J/Kg/k)	4187	4380	4270	4390
Thermal conductivity (W/mK)	0.667	0.982	0.723	1.232
Viscosity	0.415X 10^{-6}	0.63X10^{-6}	0.68X10^{-6}	0.62X10^{-6}

2.1.3SOLVER SET UP

Flow -3D, single phase and steady flow

Solver -Pressure based solver

Solution -SIMPLE

SIMPLE algorithm is used and gauss seidal numerical method is used for iteration. The solver is initialized after finalizing the boundary conditions

Table - 2 Boundary conditions

S.No	Boundary type	Boundary conditions
1	Inlet	Mass flow inlet
2	Wall	Stationary, No slip
3	Outlet	Pressure outlet
4	Inner rod	Heat load
5	Twisted strip	Stationary, no slip
6	Fluid Zone	Liquid zone

2.1.4. Solar Load Model: Solar load model is applied for numerical simulation, where typical inputs include day and time of the experiment and longitude and latitude of location. ANSYS FLUENT provides a model that can be used to calculate radiation effects from the sun's rays that enter a computational domain. It allows simulating solar loading effects and determining the solar transmission through all glazed surfaces over the course of a day. Surface-to-surface radiation model is applied for modeling the radiation mode of heat transfer between diffuse surfaces involved in the system.

2.1.5. Boundary Condition: Boundary conditions are applied for carrying out numerical simulation. For numerical simulation of Nano fluid based solar collector some boundary conditions must be imposed. The flow at the inlet was maintained as uniform mass flow at ambient temperature conditions. A low Reynolds number is typical for Heat Coefficient Enhancement applications for Parabolic Trough Collectors. This variation is due to highly temperature dependent viscosity. The inside diameter region is modeled by assuming it to be a hybrid nanofluid with very high viscosity and the velocity components have been fixed at zero value. The outlet is maintained to be at ambient pressure.

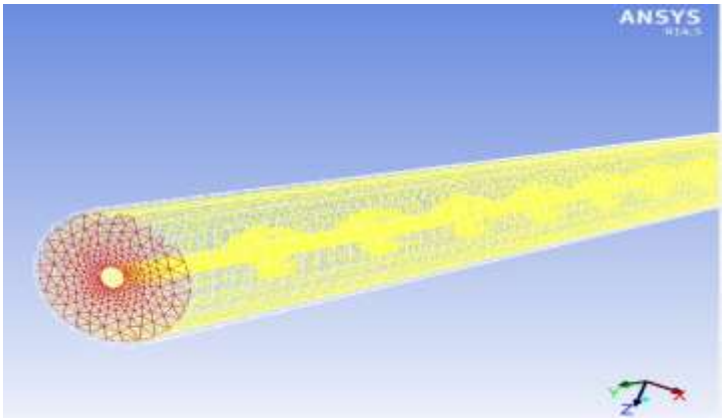

Figure 2. Grid Geometry of an absorber tube

2.1.6Ansys-Fluent Setup: The first steps taken after importing the mesh geometry into ANSYSFLUENT involve checking the mesh/grid for errors. Checking the grid assures that all zones are present and all dimensions are correct. It is also important to check the volume and make sure that it is not negative. If the volume is shown as negative, there is a problem with the grid. When the grid is checked completely and free of errors, a scale and units can be assigned. For this study, the grid was created in mm, and then scaled to meters. Once the grid was set, the solver and boundary conditions of the system were then set and cases were run and analyzed.

2.1.7 Defining The Models: To run the cases, the model properties must be set. Model properties include the internal ANSYSFLUENT solver settings like air and thermal properties, as well as model operating conditions and grid boundary conditions. The following settings were used to create the model in ANSYSFLUENT.

2.1.8 Defining the Material Properties: This section of the input contains the options for the materials to be chosen for the hybrid nanofluid is passing in the tube with hot condition. Properties that can be specified in this section are density, viscosity, specific heat, and thermal conductivity. Hybrid nanofluid is passed through the tube and due to the heat transfer from parabolic surface the hybrid nanofluid gets heated up.

Figure3: 3D Overview of Plain Tube.

For natural convection cases, density is the driving mechanism for air motion. In ANSYS-FLUENT different density models can be incorporated. Since for the present project the temperature variations should be there from start point to end point, thus the properties viscosity, specific heat and thermal conductivity are considered varying with temperature. Polynomialcurve fit equations are incorporated in ANSYS-FLUENT for varying properties.

2.1.9 Defining the Operating Conditions

The operating conditions include gravity and pressure. Gravity can be entered in values of m/s^2 in x and y and z components. In this project, the geometry was modeled assuming hybrid nanofluid will be placed on the ground with varying flows on acting downwards in the Z direction.

2.1.10. Defining the Boundary Conditions

Proper specification of the boundary conditions is a vital step in accurately modeling hybrid nanofluid flow system. In ANSYS-FLUENT, boundary conditions must be specified at each surface defined in the mesh generation process. Specifically, information about the mass flow rate, velocity and temperature must be specified at each surface. For surfaces that have been defined as “walls,” for tubeis considered as adiabatic walls with same heat flux. For surfaces that have been defined as “mass flow inlets” are specified with corresponding flow rates in to the tube. For the surfaces defined with “velocity inlets” are specified as negative velocities coming out of tube. Negative velocities are computed based on the continuity equation. For the modeling performed in this study, the boundary conditions are summarized in Table 1. Once all the models, operating conditions and boundary conditions are specified, the ANSYSFLUENT code can be executed.

Table -3 Boundary condition specification for ANSYS-FLUENT

S.No	Zone	Type	Boundary Conditions
1	Tube	Wall	Heat flux=760.020 w/m^2
2	Inlet	temperature	Heat inlet Temperature = 53ºC
3	Mass	Flow rate Inlet	0.0092,0.0157,0.046,0.05 kg/s
4	Pressure	Outlet	101395.8Pa

2.1.11. Executing the Ansys-Fluent Code

Each case must be initialized before the ANSYS-FLUENT code begins iterating toward a converged solution. Initializing the case essentially provides an initial guess for the first iteration of the solution. In the initialization process, the user must specify which zones will be provided with initial conditions. For the modeling performed in this study the option chosen was to compute from inlet. The final initialization step is for the user to enter the maximum number of iterations, after which the simulation begins. For the modeling performed in this study, the number of iterations ranged between 500 and 1000 depending on the case being run and how long it took to converge the solution.

3. DESCRIPTION OF THE PROBLEM AND GEOMETRY

The primary goal of the present work is to enhance the heat transfer in a tube employing various inserts. Also determine average Nusselt number and friction factors for Reynolds number ranging from 6000-14000 in the turbulent region. Average Nusselt numbers, friction factors of working fluid (hybrid nanofluid) flowing in the plain tube are compared with average Nusselt numbers, friction factors of working fluid (hybrid nanofluid) flowing in tube with inserts of plane twisted strip and horizontal left right twisted strip inserts which enhance heat transfer enhancement Efficiencies is compared.

CFD techniques used to perform the overall performance and optimization analysis of the fluid flow transfer of the tube with/without insert was performed using ANSYS-FLUENT.

1) Grid Info (without inserts): Cells: 93758, Nodes: 27252, Faces: 19028

Fig:4: Grid for the Absorber tube with out insert configuration

2) Grid Info (with inserts of Y=4): Cells: 1465691,Nodes: 456545,Faces: 2345636

We have also refined mesh to a finer mesh and observed that results obtained didn't have much difference, so we have considered above grid size to be optimal one for present analysis

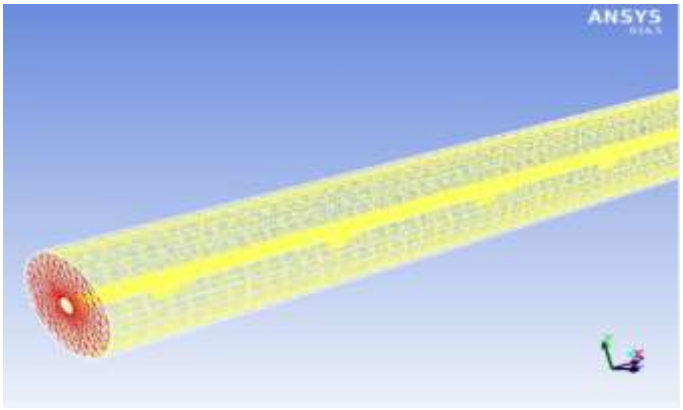

Fig:5: Grid for the Absorber tube with twisted tape of y=4 insert configuration

3) Grid Info(with inserts of Y=5.22): Cells: 1465691,Nodes: 468166,Faces: 2352312

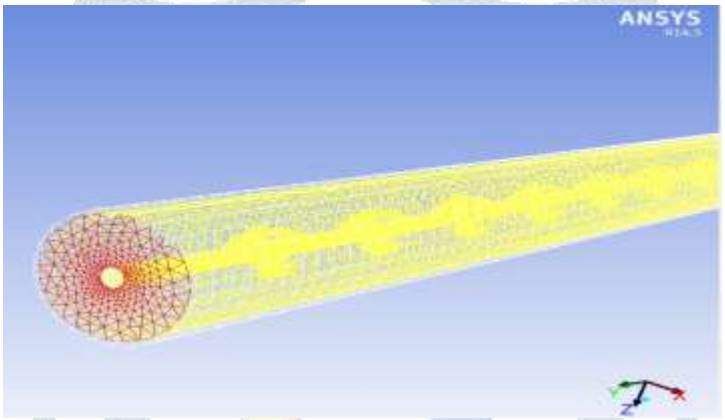

Fig:6: Grid for the Absorber tube with twisted tape of y=5.22 insert configuration

4. ANALYSIS OF PROBLEM IN ANSYS-FLUENT

Sequence of steps involved in ANSYS-FLUENT and analysis:

A. Determination of Mean Velocity (V) of working fluid (air) by using Reynolds Number considered from the following Eq...

$$Re=\rho VDi/\mu \quad \text{(i)}$$

B. Nusselt number and friction factor are calculated by equations are given below:

$$Nu=hDi/k \quad \text{(ii)}$$

$$h=((Q/A)/(Tw-Tb)) \quad \text{(iii)}$$

Where Tw= Average Surface Temperature

$$Tb=(T_i+T_0)/2 \quad \text{(iv)}$$

$$f=((\Delta P)/(L/D)\ \rho V^2/2) \quad \text{(v)}$$

C. Enhancement Efficiency is calculated using the following equation:

$$\text{Friction factor ratio} = (Nu/Nu0)/(f/fo)^{1/3} \quad \text{(vi)}$$

D. Theoretical Calculations

Nusselt number and friction factor are calculated for Reynolds numbers ranging from 6000-14000 by using DITTUS-BOELTER results are tabulated below:

Nusselt number:

$Nu=0.023 \text{ X } Re^{0.8}\text{X } Pr^{0.4}$ for $6000 \leq Re \leq 14000$ (vii)

Friction factor:

$\mathbf{f=}$ $[1.82 \log_{10} Re-1.64]^{-2}$ for $6000 \leq Re \leq 14000$ (viii)

Table 4: Theoretical Calculations

S.No	Re	f	Nu
1	2221.4	0.0452	24.3
2	4251.6	0.0405	26.2
3	5524.8	0.0398	32.4
4	8123.4	0.0356	39.3
5	9245.3	0.0352	42.1

4.1. Ansys-Fluent Calculations

In ANSYS-FLUENT also cases are analyzed separately one for plain tube, other for tube with Turbulators like Twisted tape inserts with twist ratio Y=4.0 & 5.22 respectively. The calculations for these cases are tabulated below.

Table 5: Plain Tube Calculations in ANSYS-FLUENT

S.No	Mas flow rate (Kg/s)	T_w (Avg Wall Temperature)K	T_b(K)	Q/A	Re	Nu	Pressure drop ΔP(Pa)	Heat flux h(w/m^2-K)	f
1	0.0092	350.725	328.2	759	2221.4	24.3	12.11	25.4252	0.0452
2	0.0157	344.38	325.6	759	4251.6	26.2	17.12	29.9745	0.0405
3	0.046	343.061	324.5	759	5524.8	32.4	21.82	33.5852	0.0398
4	0.05	340.36	324.2	759	8123.4	39.3	26.37	36.8925	0.0356

Table 6: Plain Tube with twisted tape (Y=4) Calculations in ANSYS-FLUENT

S.No	Mas flow rate (Kg/s)	T_w (Avg Wall Temperature)K	T_b(K)	Q/A	Re	Nu	Pressure drop ΔP(Pa)	Heat flux h(w/m^2-K)	f
1	0.0092	348.61	328.2	759	2221.4	32.4	48.11	31.49321	0.1489
2	0.0157	346.18	325.6	759	4251.6	35.6	69.12	39.54624	0.1462
3	0.046	345.42	324.5	759	5524.8	42.5	88.82	42.85061	0.1387
4	0.05	344.84	324.2	759	8123.4	47.4	106.37	48.54782	0.1342

Table 7: Plain Tube with twisted tape (Y=5.22) Calculations in ANSYS-FLUENT

S.No	Mas flow rate (Kg/s)	T_w (Avg Wall Temperature)K	T_b(K)	Q/A	Re	Nu	Pressure drop ΔP(Pa)	Heat flux h(w/m^2-K)	f
1	0.0092	349.52	328.2	759	2221.4	34.2	49.37	32.28414	0.1923
2	0.0157	352.98	325.6	759	4251.6	37.8	71.34	41.46832	0.1871
3	0.046	356.12	324.5	759	5524.8	45.6	90.74	44.52475	0.1622
4	0.05	359.84	324.2	759	8123.4	49.2	108.46	50.73559	0.1421

5. CFD RESULTS AND ANALYSIS

Each case was run using higher order residual schemes for each governing equations. It was ensured that residuals dropped to at least 10-6 for each case. Nusselt number and friction factor for plain tube are validated with theoretical relations and then they are determined for twisted tape inserts. Nusselt number and friction factor calculated for the plain tube and plain tube with different insert for 6000<Re<14000. The Nusselt number and friction factor obtained for the tube with insert are compared with Nusselt number and friction factor of Plain tube. Each case is solved for 3 equations Energy, Momentum and Turbulence and results are plotted on corresponding graphs as shown below.

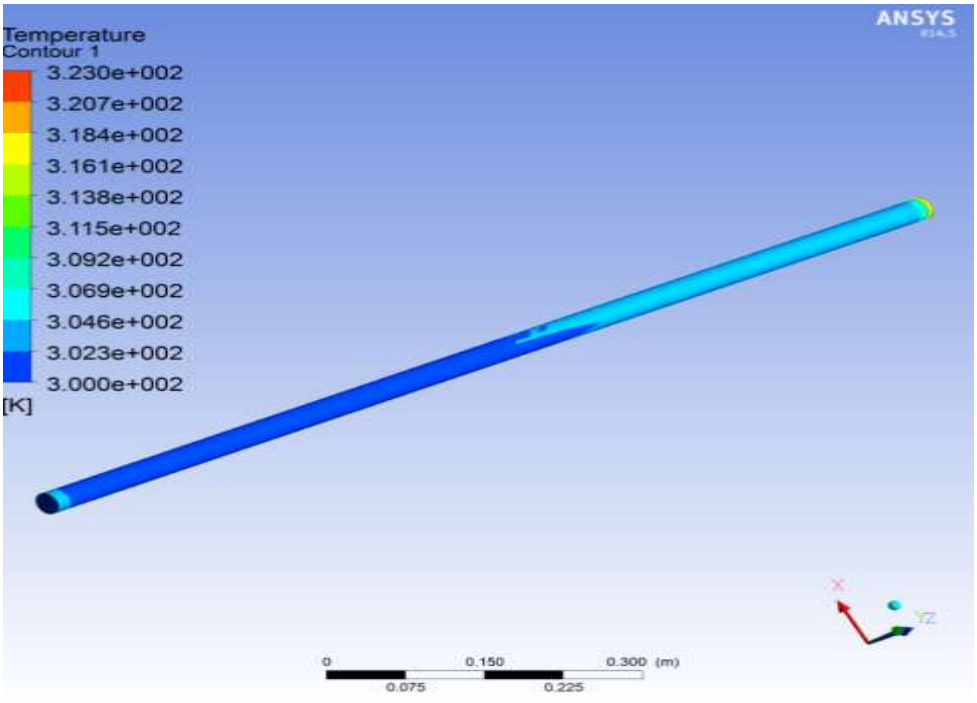

Fig 7: Static Temperature Variations for the Plain Tube configuration with DI-water

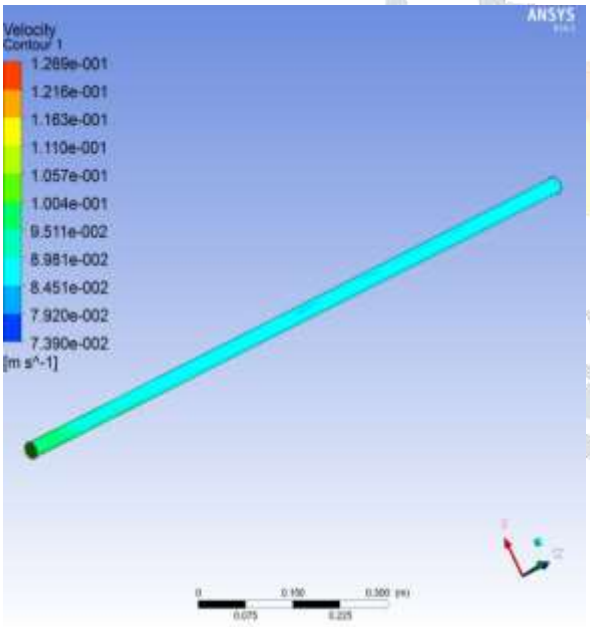

Fig 8: Velocity Variation for the Plain Tube configuration with DI-water

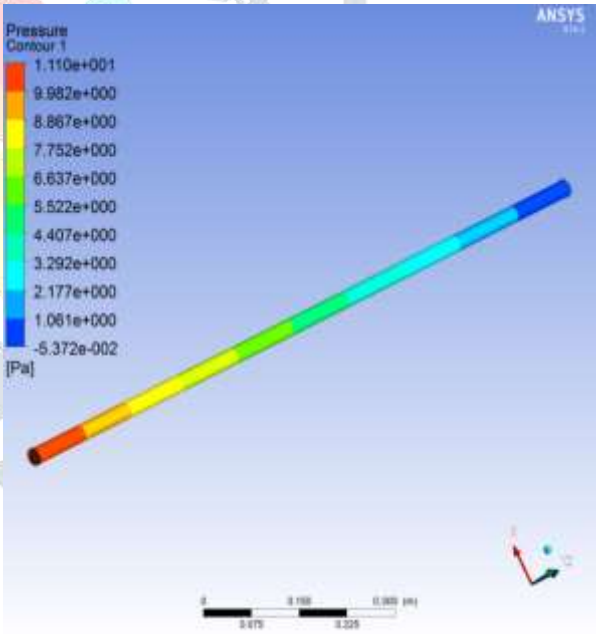

Fig 9: Pressure Variation for the Plain Tube configuration with DI-Water

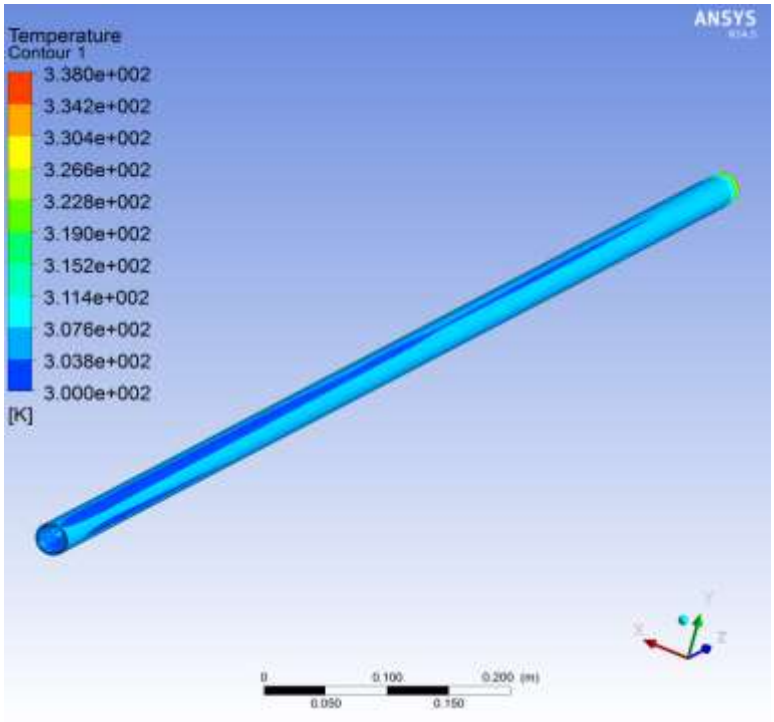

Fig 10: Static Temperature Variations for the Plain Tube configuration with TiO_2 + DI-water

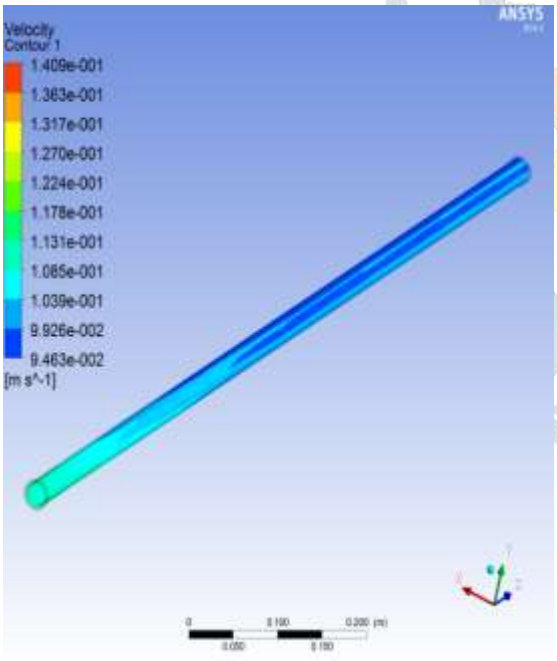

Fig 11: Velocity Variation for the Plain Tube configuration with TiO_2 + DI-water

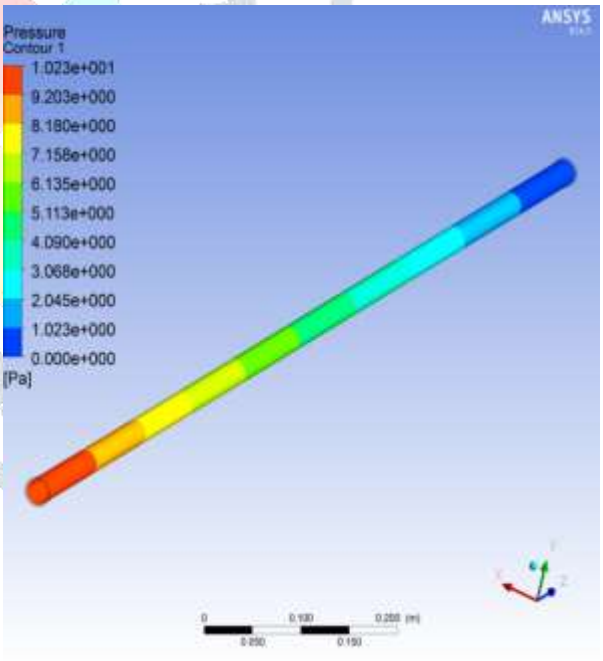

Fig 12: Pressure Variation for the Plain Tube configuration with TiO_2 + DI-water

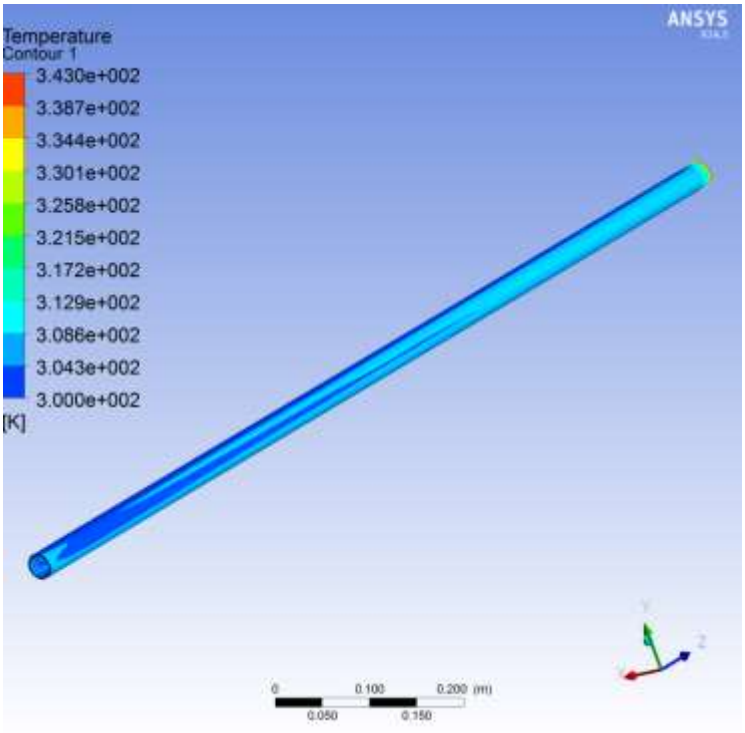

Fig 13: Static Temperature Variations for the Plain Tube configuration with GO + DI-water

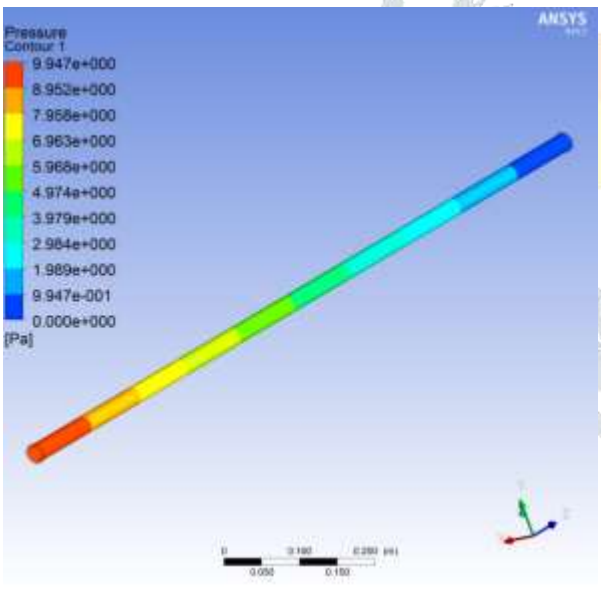

Fig 14: Velocity Variation for the Plain Tube configuration with GO + DI-water

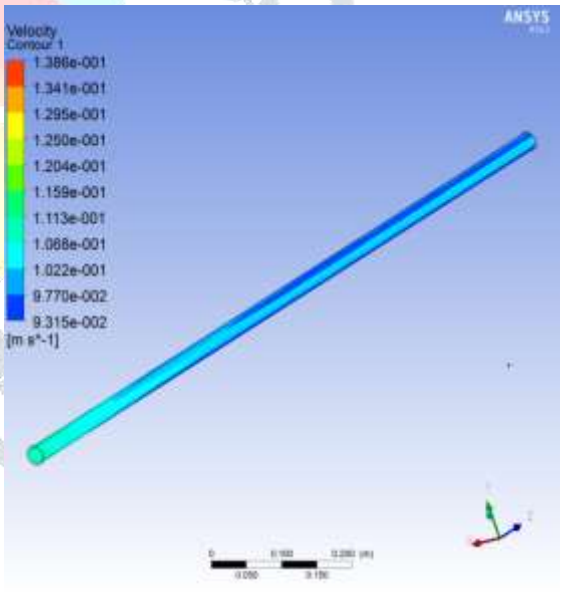

Fig 15: Pressure Variation for the Plain Tube configuration with GO + DI-water

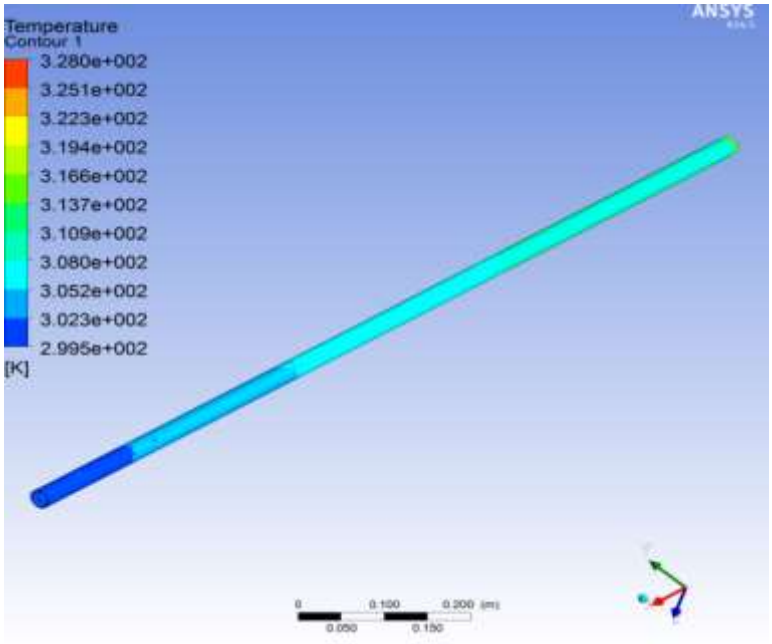

Fig 16: Temperature Variation for the Tube with Twisted tape insert configuration Y=4 for DI-Water

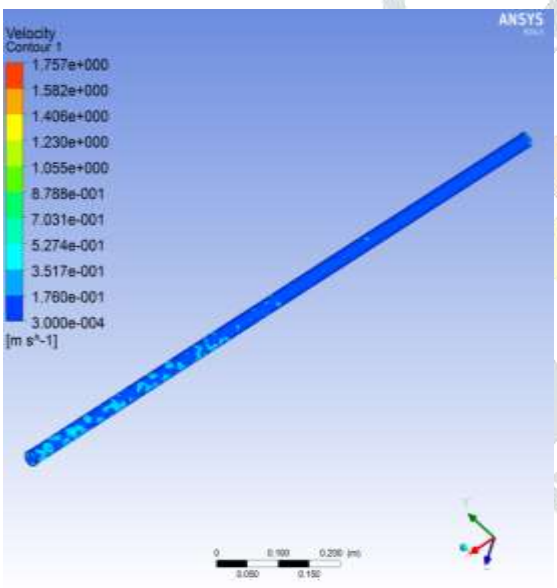

Fig 17: Velocity Variation for Tube with Twisted tape insert configuration Y=4 for DI-Water

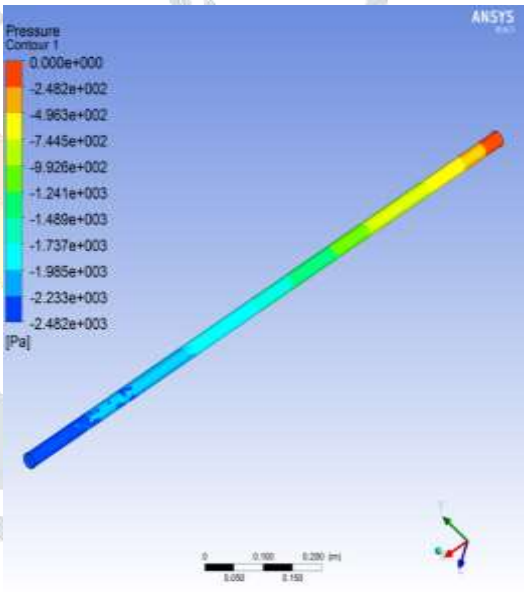

Fig18: Pressure Variation for the Tube with Twisted tape insert configuration Y=4 for DI-Water

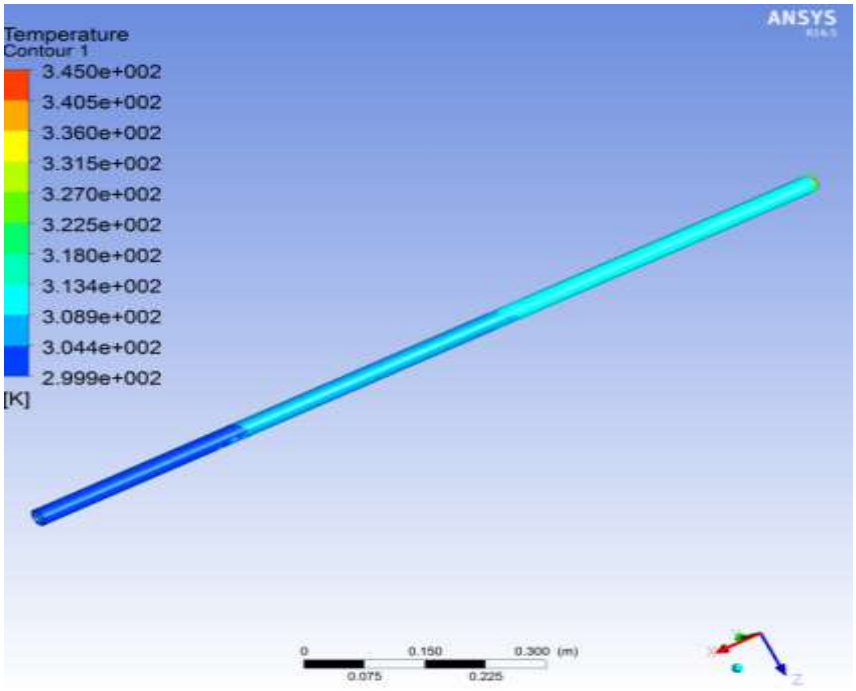

Fig 19: Temperature Variation for the Tube with Twisted tape insert configuration Y=4 for TiO_2+DI-Water

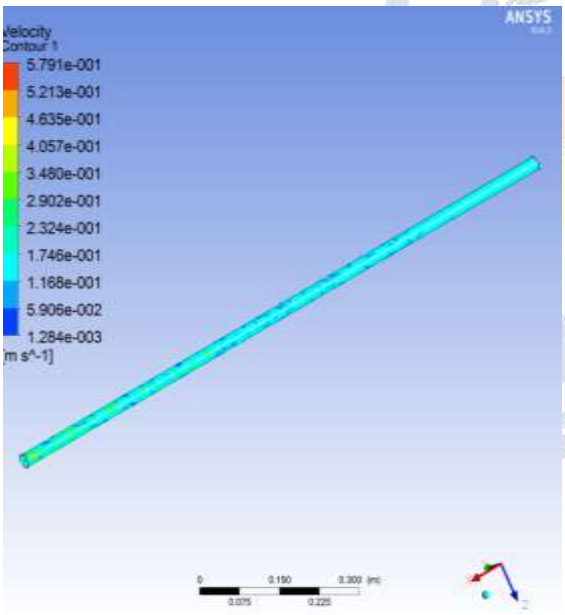

Fig 20: Velocity Variation for Tube with tape insert configuration Y=4 for Water

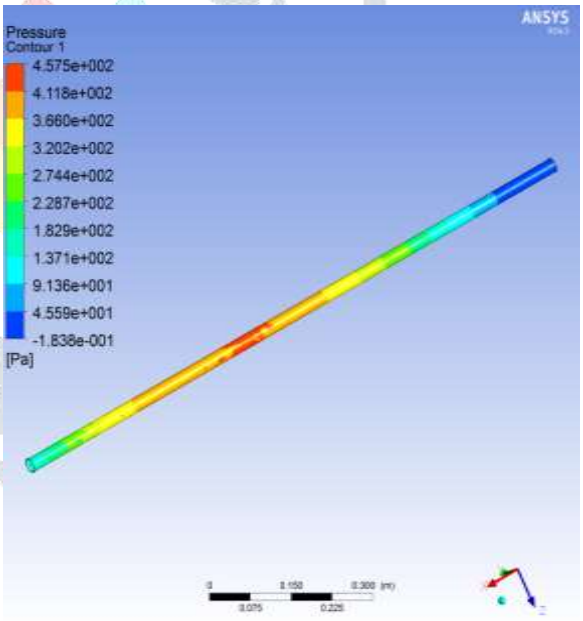

Fig 21: Pressure Variation for the Tube Twisted Twisted tape insert configuration Y=4 for withTiO_2 +DI- TiO_2+DI-Water

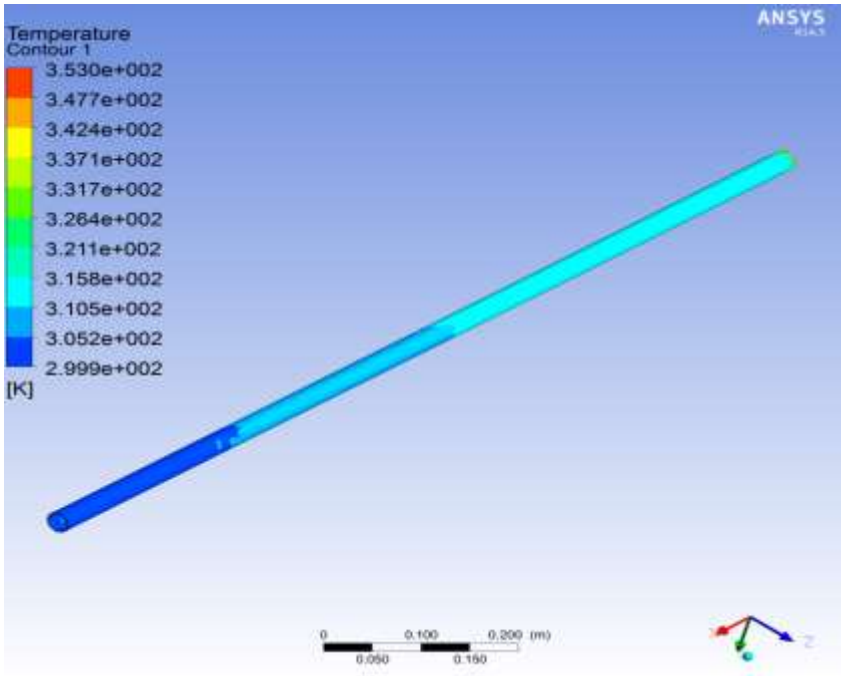

Fig 22: Temperature Variation for the Tube with Twisted tape insert configuration Y=4 for GO+DI-Water

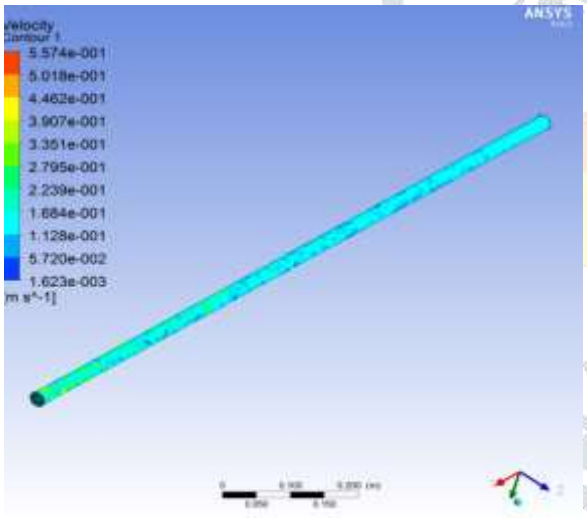

Fig 23: Velocity Variation for the Tube with Twisted tape insert configuration Y=4 for GO + DI-Water

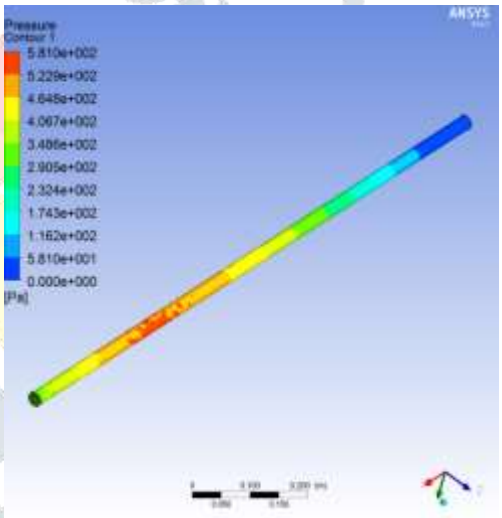

Fig 24: Pressure Variation for Tube with Twisted tape insert configuration Y=4 for GO + DI-Water

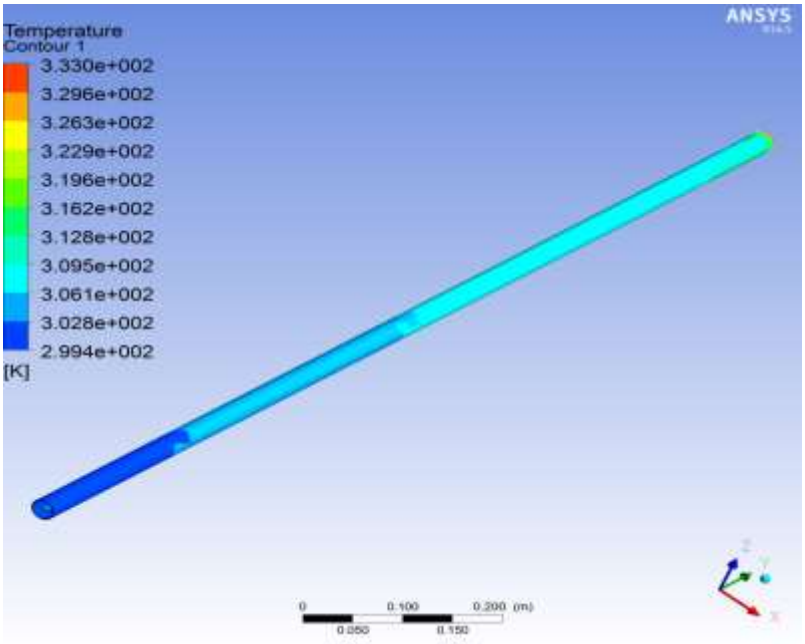

Fig 25: Temperature Variation for the Tube with Twisted tape insert configuration Y=5.22 for DI-Water

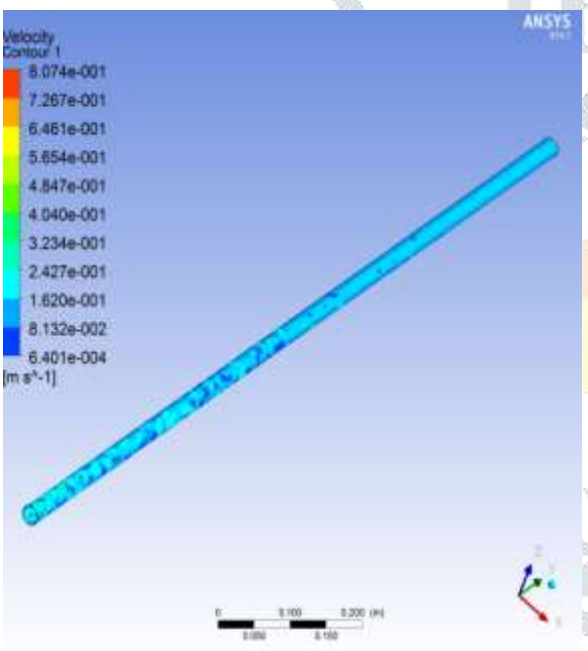

Fig 26: Velocity Variation for Tube with insert configuration Y=5.22 for DI-Water

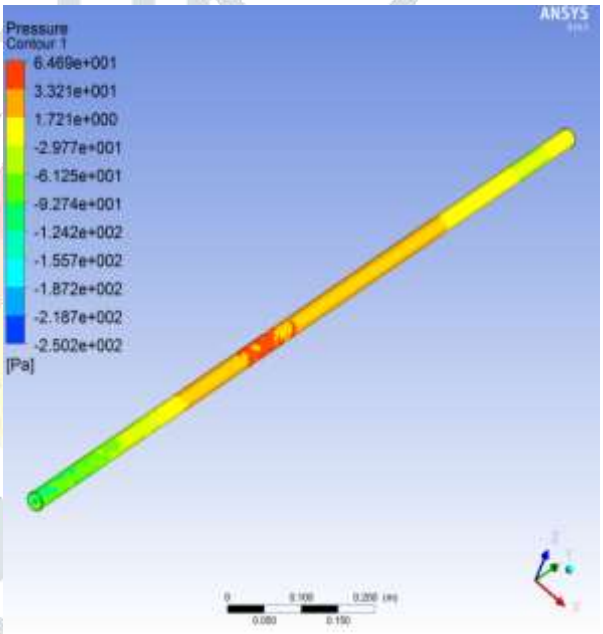

Fig 27: Pressure Variation for the Tube Twisted tape with Twisted tape insert configuration Y=5.22 for DI-Water

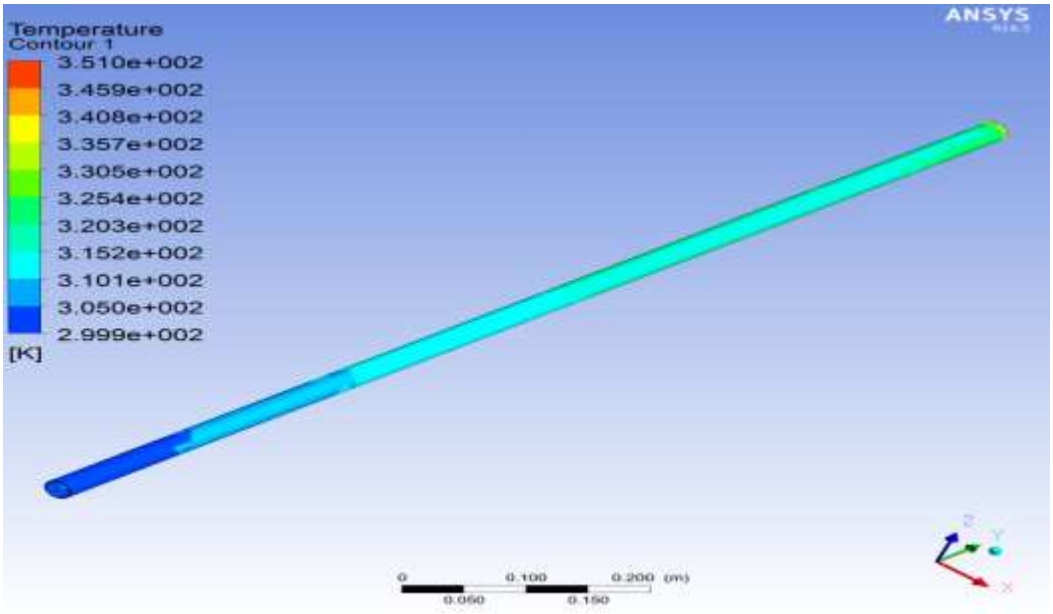

Fig 28: Temperature Variation for the Tube with Twisted tape insert configuration Y=5.22 for TiO_2+DI-Water

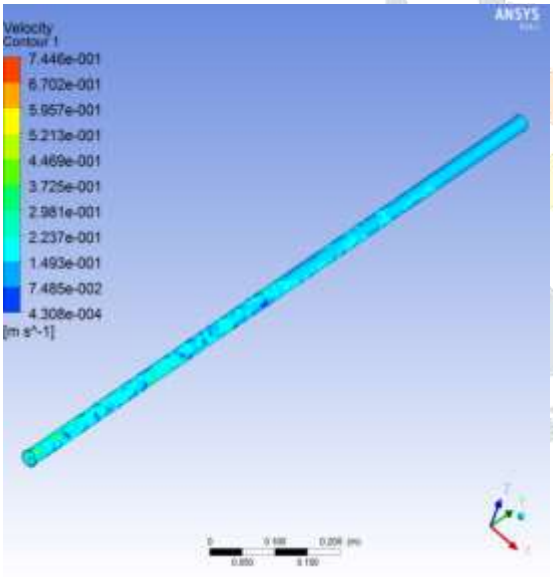

Fig 29: Velocity Variation for Tube with Twisted tape insert configuration Y=5.22 for TiO_2+DI-Water

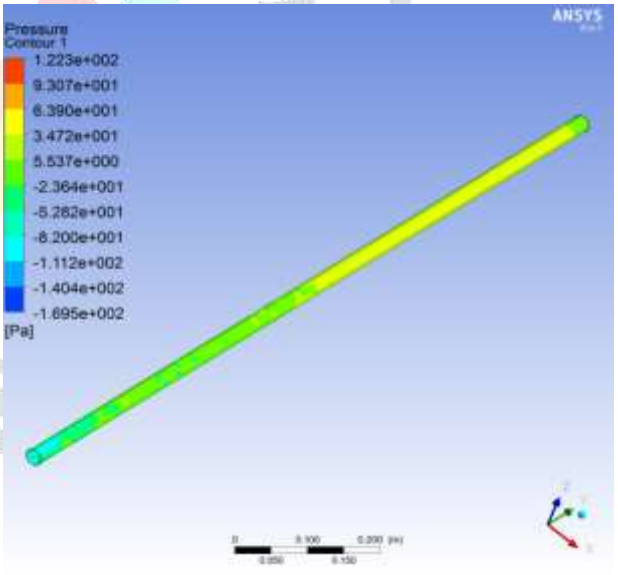

Fig 30: Pressure Variation for the Tube With Twisted tape insert configuration Y= 5.22 forTiO_2 +DI-Water

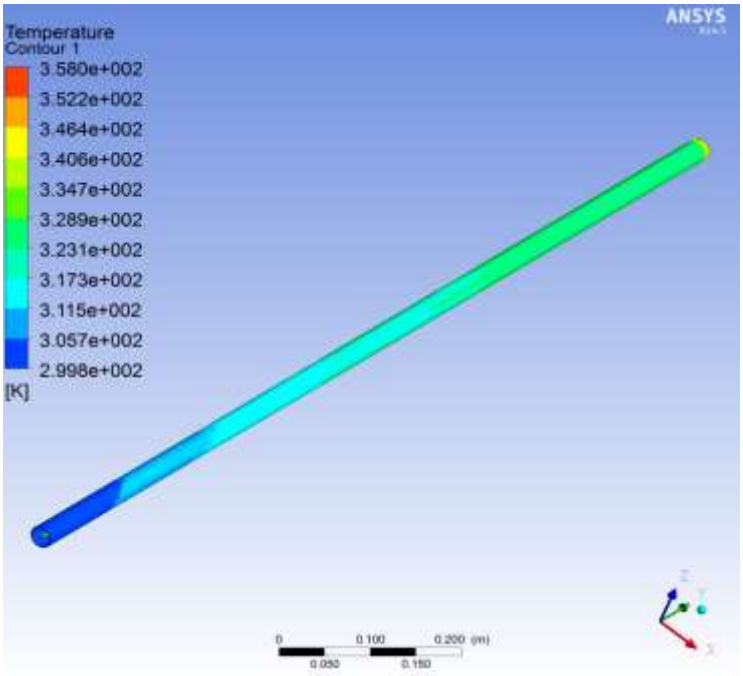

Fig31: Temperature Variation for the Tube with Twisted tape insert configuration Y=5.22 for GO+DI-Water

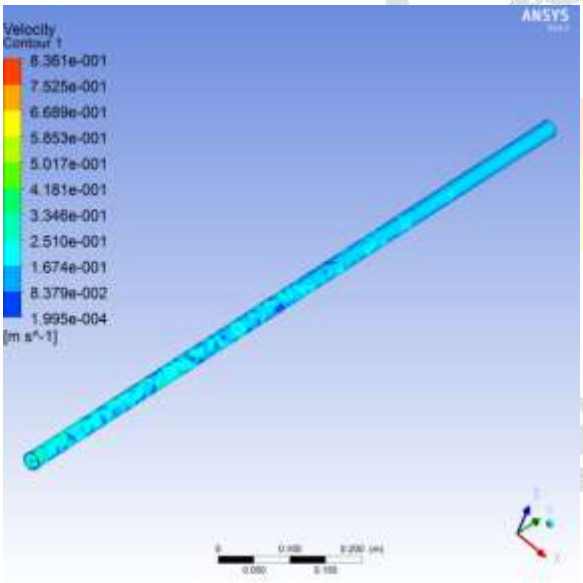

Fig 32: Velocity Variation for Tube with Twisted tape insert configuration GO+DI-Water

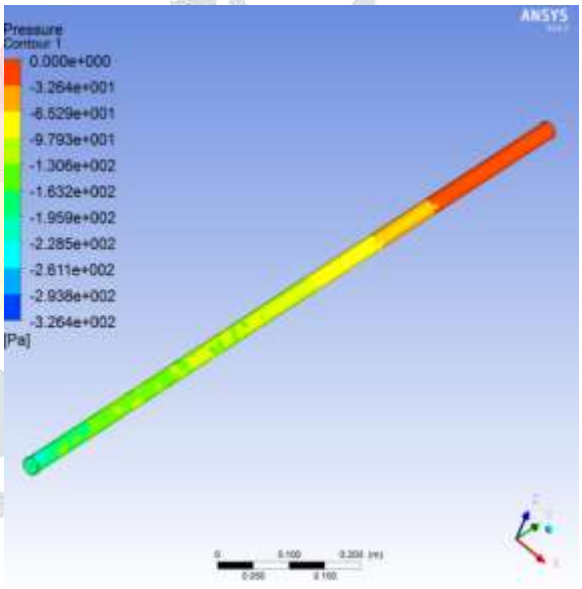

Fig 33: Pressure Variation for the Tube With Twisted tape insert configuration Y=5.22 for Y=5.22 for GO+DI-Water

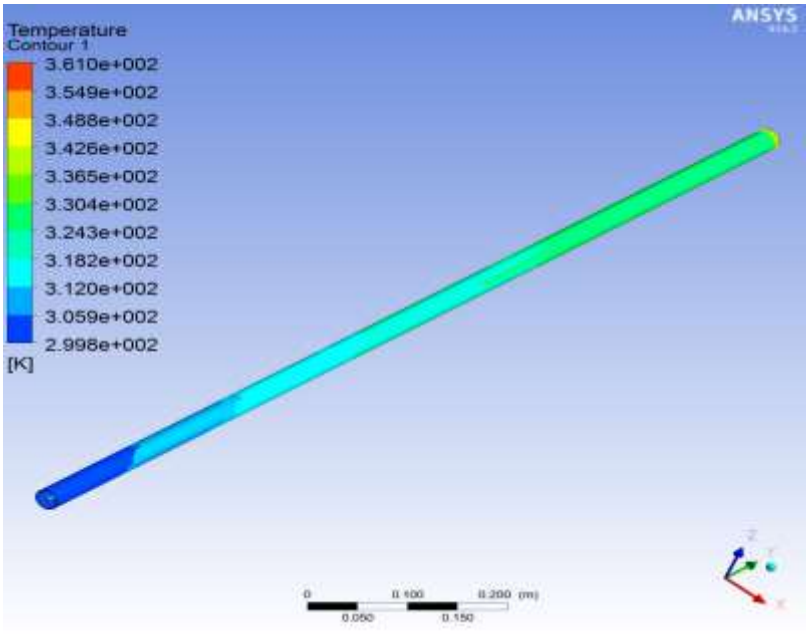

Fig 34: Temperature Variation for the Tube with Twisted tape insert configuration Y=5.22 for GO+TiO_2 DI-Water (HYBRID)

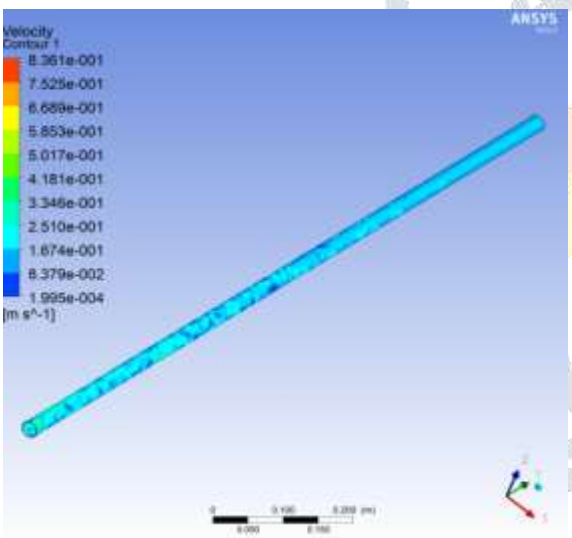

Fig 35: Velocity Variation for Tube with Twisted tape insert configuration Y=5.22 for GO+TiO_2+DI-Water (HYBRID)Y=5.22

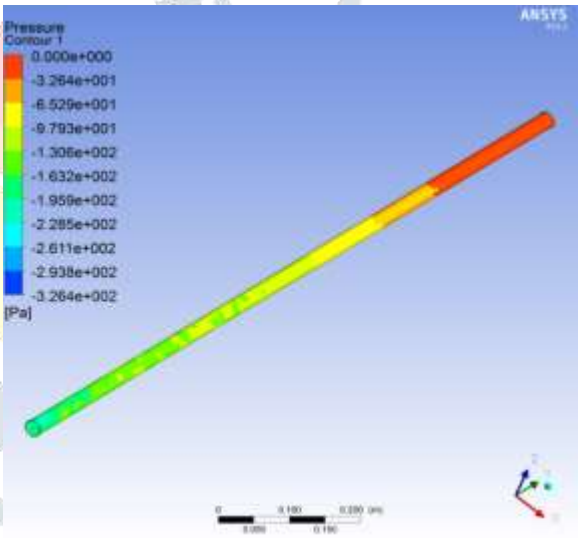

Fig 36: Pressure Variation for Tube With Twisted tape insert configuration for GO+TiO_2+DI-Water (HYBRID)

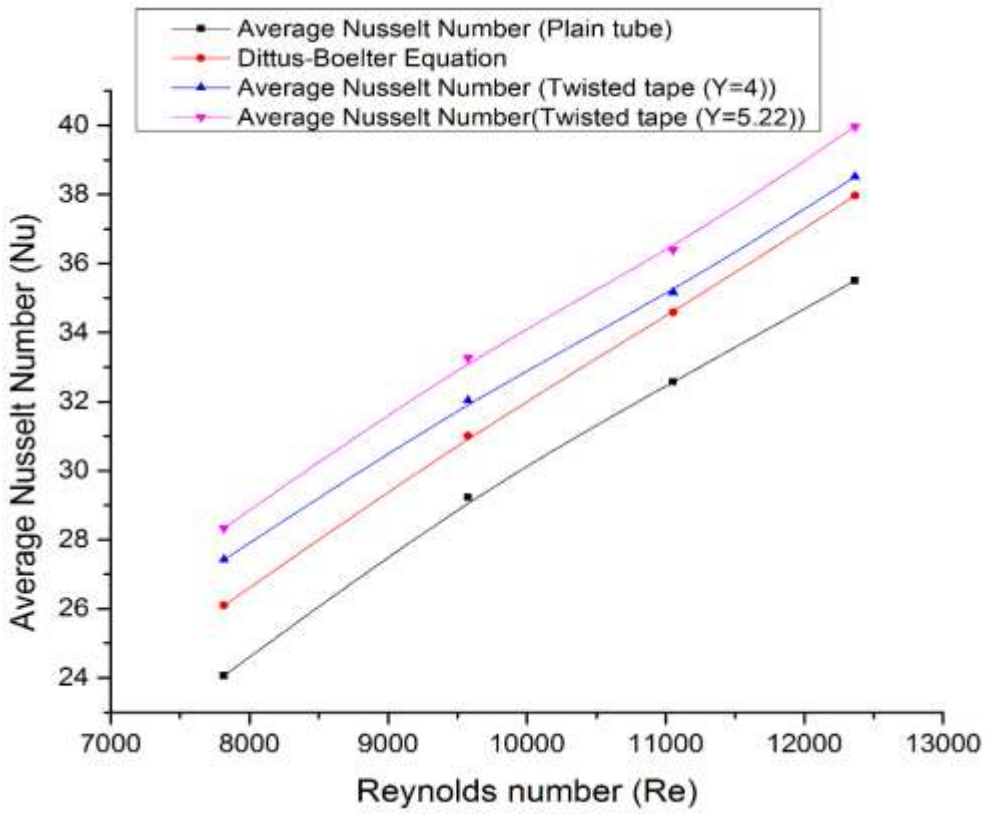

Fig 37: Variation of Nusselt Number Vs Reynolds number.

Comparison graph between Theoretical and CFD Analysis for Variation of Average Nusselt Number with Reynolds number in Plain Tube and twisted tape tube with Y= 4 & 5.22.

A. Inference from Graph

Above graph reveals that results obtained through Flunet 6.3 are almost identical with values thorugh DITTUS-BOELTER Equation for Nusselt number. The Maximum % variation of CFD results for Nusslet number is found to be 8.1% with respect to theoretical values for plain tube. The maximum % variation of CFD results for Nusselt Number is found to 35% with respect to Plain Tube with inserts Y=4 & 5.22.

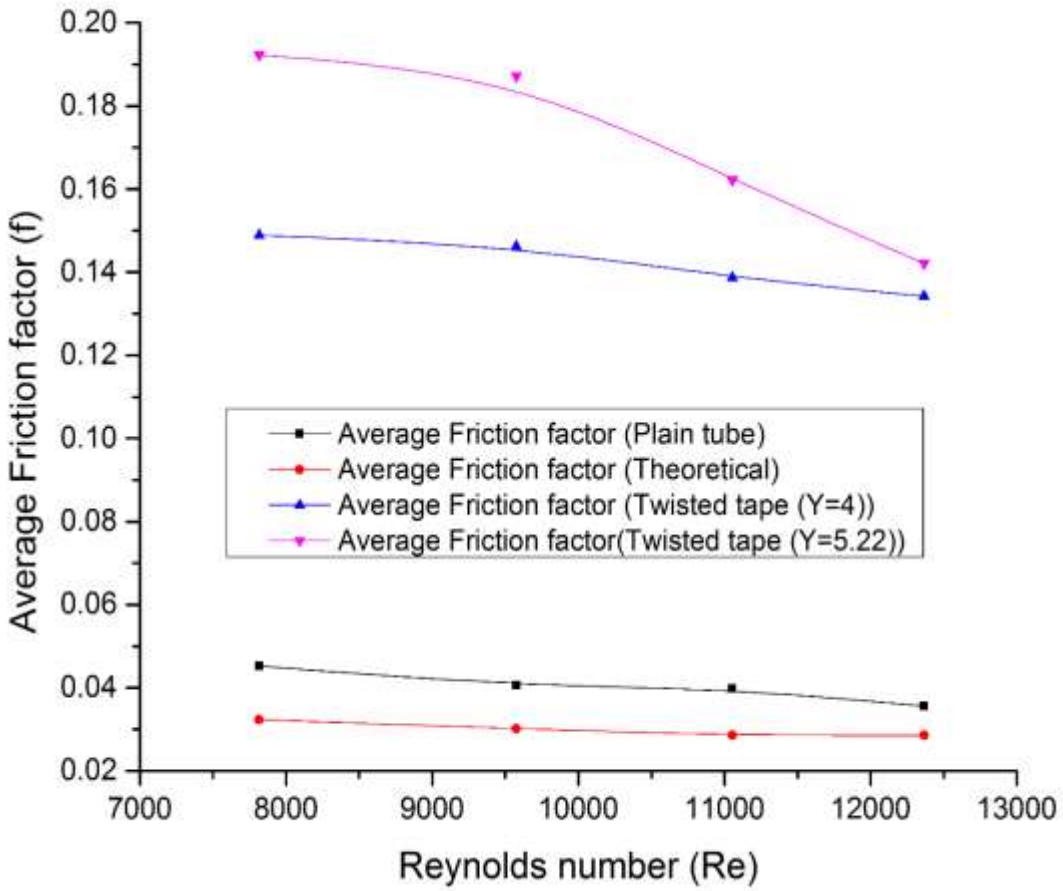

Fig 38: Variation of Friction Factor Vs Reynolds number.

Comparison graph between Theoretical and CFD Analysis for Variation of Friction Factor with Reynolds number in Plain Tube, twisted tape inserts with Y=4 & 5.22. Inference from Graph Above graph reveals that results obtained through Flunet 6.3 are well within the range of values obtained through DITTUSBOELTER Equation for Friction Factor. The Maximum % variation of CFD results for Friction Factor is found to be 10.2% with respect to theoretical values. The max % variation of CFD results for Friction factor is found to 308% with respect to Plain Tube with inserts Y= 4& 5.22.

B. Inference From Graph

From the graph reveals that results obtained through Fluent 6.3. Comparison graph between the Nusselt Number Vs Reynolds Number of CFD values of Twisted tape insert thru Fluent 6.3.

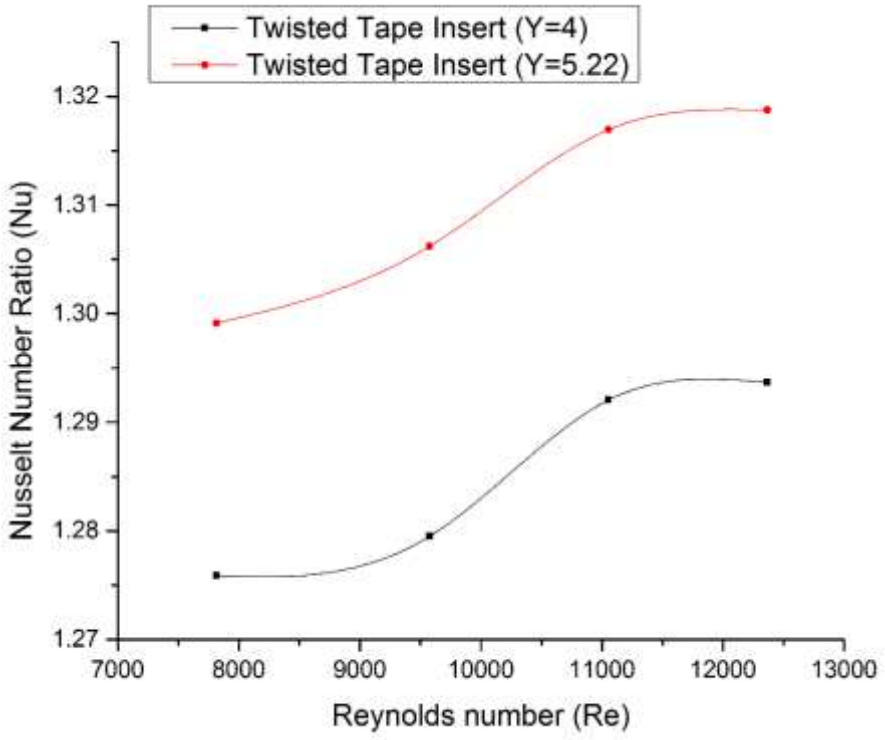

Fig 39: Nusselt Number Vs Reynolds Number

Above graph reveals that if Reynolds number increases Nusselt number ratio also increasing. Maximum Enhancement of Nusselt Number for Twisted tape insert= 1.296.

C. Inference From Graph

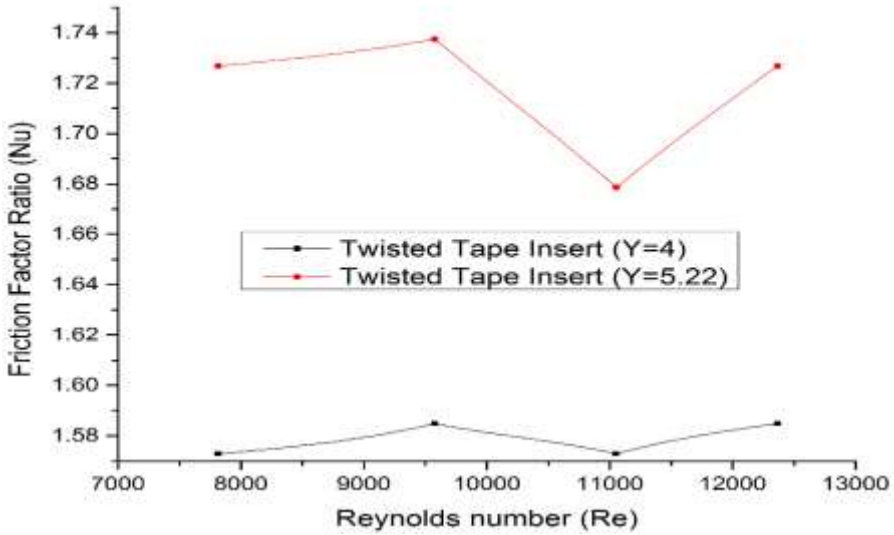

Fig 40: Friction Factor Vs Reynolds Number.

Comparison graph between the Friction Factor Vs Reynolds Number of CFD values of Twisted tape insert thru Fluent 6.3. Above graph reveals that if Reynolds number increases friction factor is decreasing. Minimum friction factor ratio of Twisted tape insert = 1.723.

D. Inference From Graph

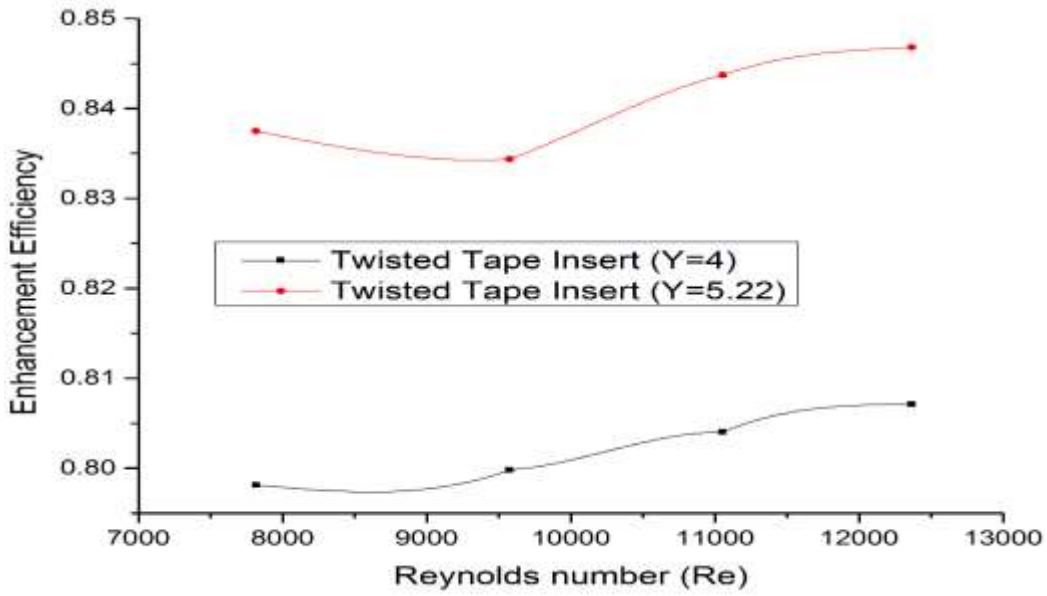

Fig 41: Enhancement Efficiency Vs Reynolds Number

Comparison graph between the Enhancement Efficiency Vs Reynolds Number of CFD values Twisted tape insert thru Fluent 6.3.

E. Inference From Graph

Above graph reveals that if Reynolds number increases Enhancement efficiency also increasing. Maximum enhancement efficiency of Twisted tape insert= 0.845

6. CONCLUSION

In the present work CFD Analysis of enhancement of heat transfer of twisted strip insert for improving heat transfer in Horizontal tube has been carried out with boundary conditions such as mass inlet and pressure outlet having defined with constant heat flux. Mesh is created by taking symmetric model in Gambit 2.2.30 (3- dimensional). The variations of Temperatures, average Nusselt Numbers, friction factor and pressure drop on with insert like twisted have been studied.

Reluts revelaed that average Nusselt Numbers and friction factor are considerably more with maximum enhancement efficiency ratio of 0.845 for Twisted tape insert when compared to plain tube. Improvement of Average Nusselt Numbers for tube with Twisted tape insert is found that to be 41% when compared to

plain tube. Similarly, friction factor for tube with Twisted tape insert is found that to be 32% when compared to plain tube

REFERENCES

[1] R.C. Prasad, J. Shen, Performance evaluation of convective heat transfer enhancement devices using exergy analysis, International Journal of Heat and Mass Transfer 36 (1993) 4193–4197

[2] R.C. Prasad, J. Shen, Performance evaluation using exergy analysis–application to wire-coil inserts in forced convection heat transfer, International Journal of Heat and Mass Transfer 37 (1994) 2297–22303.

[3] T.S. Ravigururajan, A.E. Bergles, Development and verification of general correlations for pressure drop and heat transfer in single-phase turbulent flow in enhanced tubes, Experimental Thermal and Fluid Science 13 (1996) 55–70. 762 P. Naphon / International Communications in Heat and Mass Transfer (2006) 753–763

[4] K.N. Agrawal, A. Kumar, M.A.A. Behabadi, H.K. Varma, Heat transfer augmentation by coiled wire inserts during forced convection condensation of R-22inside horizontal tubes, International Journal of Multiphase Flow 24 (1998) 635–650

[5] H.Y. Kim, S. Koyama, W. Matsumoto, Flow pattern and flow characteristics for counter-current two-phase flow in a vertical round tube with wire-coil inserts, International Journal of Multiphase Flow 27 (2001) 2063–2081.

[6] L. Wang, B. Sund, Performance comparison of some tube inserts, International Communication Heat Mass Transfer 29 (2002) 45–56.

[7] H.R. Rahai, T.W.Wong, Velocity field characteristics of turbulent jets from round tubes with coil inserts, Applied Thermal Engineering 22(2002) 1037–1045.

[8] V. Ozceyhan, Conjugate heat transfer and thermal stress analysis of wire coil inserted tubes 0 that are heated externally with uniform heat flux, Energy Conversion and Management 46 (2005) 1543–1559.

[9] R.L. Webb, R. Narayanmurthy, P. Thors, Heat transfer and friction factor characteristics of internal helical-rib roughness, Trans. ASME J. Heat Transfer 122 (2000) 134–142.

[10] S.U.S. Choi, Enhancing thermal conductivity of fluid with nanoparticles, in: D.A. Siginer, H.P. Wang (Eds.), Developments and Applications of Non- Newtonian Flows, FED-V.231/MD-V.66, vol. 66, ASME, New York, 1995, pp. 99–105.

[11] Yun, J. Hwang, J.T. Chung, Y. Kim, Flow boiling heat transfer characteristics of nitrogen in plain and wire coil inserted tubes, Int. J. Heat Transfer 50 (2007) 2339–2345.